

Roberto C. Gallo-Villanueva<sup>1</sup>  
 Carlos E. Rodríguez-López<sup>1</sup>  
 Rocío I. Díaz-de-la-Garza<sup>2</sup>  
 Claudia Reyes-Betanzo<sup>3</sup>  
 Blanca H. Lapizco-Encinas<sup>1</sup>

<sup>1</sup>Departamento de Biotecnología e Ingeniería de Alimentos y Centro de Biotecnología, Tecnológico de Monterrey, Monterrey, Nuevo León, México

<sup>2</sup>Departamento de Agrobiotecnología y Agronegocios y Centro de Biotecnología, Tecnológico de Monterrey, Monterrey, Nuevo León, México

<sup>3</sup>Departamento de Electrónica, Instituto Nacional de Astrofísica, Óptica y Electrónica, Tonantzintla, Puebla, México

Received June 2, 2009

Revised September 8, 2009

Accepted September 15, 2009

## Research Article

# DNA manipulation by means of insulator-based dielectrophoresis employing direct current electric fields

Electrokinetic techniques offer a great potential for biological particle manipulation. Among these, dielectrophoresis (DEP) has been successfully utilized for the concentration of bioparticles. Traditionally, DEP is performed employing microelectrodes, an approach with attractive characteristics but expensive due to microelectrode fabrication costs. An alternative is insulator-based DEP, a method where non-uniform electric fields are created with arrays of insulating structures. This study presents the concentration of linear DNA particles (pET28b) employing a microchannel, with an array of cylindrical insulating structures and direct current electric fields. Results showed manipulation of DNA particles with a combination of electroosmotic, electrophoretic, and dielectrophoretic forces. Employing suspending media with conductivity of 104  $\mu\text{S}/\text{cm}$  and pH of 11.15, under applied fields between 500 and 1500 V/cm, DNA particles were observed to be immobilized due to negative dielectrophoretic trapping. The observation of DNA aggregates that occurred at higher applied fields, and dispersed once the field was removed is also included. Finally, concentration factors varying from 8 to 24 times the feed concentration were measured at 2000 V/cm after concentration time-periods of 20–40 s. The results presented here demonstrate the potential of insulator-based DEP for DNA concentration, and open the possibility for fast DNA manipulation for laboratory and large-scale applications.

### Keywords:

DNA / Dielectrophoresis / Electrokinetic / Microchannel / Microfluidics

DOI 10.1002/elps.200900355

## 1 Introduction

Miniaturization has benefited numerous analytical applications, from environmental analysis, biomedical testing, food safety to drug development [1–3]. Miniaturization offers attractive advantages over traditional bench scale processes, such as shorter analysis time, reduced sample and reagent consumption, enhanced sensitivity, high resolution, and portability [4]. Microfluidic technology has advanced significantly, since it began almost two decades ago. There is a growing interest in developing separation techniques amenable for miniaturization. Electrokinetic (EK) techniques such

as electrophoresis (EP) and dielectrophoresis (DEP) are among the most employed methods in micro total analysis systems ( $\mu\text{TAS}$ ) [5].

DEP is an EK transport mechanism that allows the manipulation of particles due to polarization effects in the presence of non-uniform electric fields; it can be employed with direct current (DC) and alternating current (AC) electric fields. DEP can achieve concentration and separation on a single step, and has been successfully employed to handle a wide array of bioparticles: proteins [6–8], DNA [8–11], virus [12, 13] bacteria [14–16], yeast [17], mammalian cells [18–20], red blood cells [21], and parasites [22].

### 1.1 Importance of DNA purification

DEP manipulation of DNA particles on microscale represents a great promise for numerous analytical applications and nucleic acid large-scale production. Separation, concentration, and purification of DNA using DEP-based microdevices could become an alternative to the traditional gel EP techniques, which are time consuming, not convenient for very long DNA molecules, and generate significant biohazard waste. Moreover, the ability to separate nucleic acids with DEP while observing the process could allow the monitoring of their

**Correspondence:** Dr. Blanca H. Lapizco-Encinas, Departamento de Biotecnología e Ingeniería de Alimentos, Tecnológico de Monterrey, Campus Monterrey, Avenida Eugenio Garza Sada 2501 Sur, Monterrey, Nuevo León, 64849, México  
**E-mail:** blapizco@itesm.mx  
**Fax:** +52-818-328-1400

**Abbreviations:** AC, alternating current; CM, Clausius–Mossoti; CF, concentration factor; DC, direct current; DEP, dielectrophoresis; eDEP, electrode-based DEP; EK, electrokinetic; EP, electrophoresis; iDEP, insulator-based dielectrophoresis; TEA, triethanolamine

interactions with other molecules (*e.g.* proteins). This opens the possibility for several biotechnological analytical applications, such as on-chip hybridizations and synthesis, gene mapping and genotyping, and so on. DEP stands as an alternative method that could integrate large-scale purification and concentration of DNA particles on a single step, with the potential to replace chromatographic purification, which has been the traditional approach employed to eliminate contaminants from DNA [23–26]. In addition, the use of EOF as the fluid driving force can prevent DNA degradation caused by shear-stress generated by pressure-driven flow [27]. DEP can be envisaged as a technique that could answer many of the requirements for purification of pharmaceutical-grade nucleic acids. Gene therapy and DNA vaccines will become a commercial reality in the following years [28–30], in fact, large-scale production and purification of nucleic acids are currently on demand for both laboratory and clinical trials [31, 32]. Microdevices used in massively parallel systems could accomplish large-scale DNA purification, leading to faster separations while decreasing reagent consumption, making the purification processes more economically favorable.

## 1.2 Background on DEP manipulation of DNA particles

Recent applications of DEP for the manipulation and concentration of DNA particles [8, 33–36] demonstrate that DNA can be concentrated and separated employing DEP microdevices. However, a vast majority of the studies focused on the DEP manipulation of DNA have been achieved employing arrays of microelectrodes and AC electric fields [37]. There is a wide breath of knowledge in the usage of electrode-based DEP (eDEP). Employing electrodes allows particle manipulation with low applied voltages and many electrode geometries have been successfully tested. However, electrode fabrication is complicated and expensive, due to time-consuming metal deposition steps, making large-scale systems less economically feasible. Furthermore, electrode functionality is negatively affected by fouling, which is common when handling bioparticles [38–42]. An alternative is to employ insulating structures, instead of electrodes, to create non-uniform electric fields required for DEP. Insulator-based dielectrophoresis (iDEP) is a technique where insulating structures function as “obstacles” when applying an electric field, and their presence bends the electric field creating regions of higher and lower field intensity, *i.e.* a non-uniform field [40]. This approach has been tested to manipulate bioparticles in different systems, by employing glass beads [43], oil menisci [41], square or triangular hurdles [39], nanopipettes [34], arrays of insulating structures [7, 38, 40, 44, 45], and microchannels with sawtooth walls [46].

One of the first attempts on testing the potential of iDEP for DNA manipulation was proposed in 2002 by Chou *et al.* [38] with a microdevice that concentrated PCR-amplified ssDNA (137 nucleotides) and dsDNA (0.37, 1.1, 4.4, and

40 kbp) particles with AC electric fields [38]. This group employed a microdevice with trapezoidal insulating posts with constrictions that were 1  $\mu\text{m}$  wide. Their results showed the concentration and positive DEP trapping of 0.37 kbp DNA at the constrictions, when a voltage of 1 kV was applied, at frequencies of 200–1000 Hz. At low frequencies, there was no DEP trapping, and as the frequency increased, DNA molecules were attracted to the constrictions. They explained that at low frequencies, DNA molecules were pulled out of the DEP traps (constrictions) by EP forces. At higher frequencies, the DEP force was greater than the EP force, which allowed for the DNA molecules to become dielectrophoretically immobilized at the constrictions. It was shown that ssDNA exhibits a lower DEP force than dsDNA [38]. In 2003, Chou and Zenhausern published positive DEP manipulation of 1 kbp ssDNA employing a PDMS device [47].

The potential for size separation of DNA with length-dependent polarizabilities due to different migration velocities was first proposed in 1991 by Ajdari and Prost [48]. Following this approach, in 2007 Regtmeier *et al.* [45] reported iDEP manipulation of  $\lambda$ -DNA (48.5 kbp), T2 (164 kbp), and supercoiled covalently closed circular plasmid DNA (7 and 14 kbp), utilizing a PDMS microdevice that contained an array of rectangular insulating posts with constrictions of 2.3  $\mu\text{m}$ . They achieved fractionation of mixtures of DNA particles with positive DEP, separating 48.5 kbp linear from 164 kbp linear DNA particles, and 7 and 14 kbp covalently closed circular DNA particles. They employed DC fields to achieve migration and AC fields to achieve immobilization of DNA particles, while EOF was effectively reduced by applying a PEG-silane coating on the microdevice surface. Larger DNA particles would trap sooner than smaller particles, allowing for spatial separation of the different types of DNA. After particles were immobilized, the microdevice was scanned for fluorescence signal across its length obtaining an electropherogram with good resolution. This study presented a successful separation of a DNA mixture, and offers a great potential for analytical applications. However, high-throughput operation would require a flow-through system [49].

iDEP has also been employed for continuous sorting of DNA particles. In 2008 Parikesit *et al.* [50] reported the fractionation of a mixture of  $\lambda$ -DNA (48.5 kbp) and T4GT7-DNA (165.6 kbp) employing a microdevice made from glass that contained a very shallow microchannel (depth 400 nm), featuring a sharp U-turn. DNA particles were sorted based on the trajectory deflection induced by DEP at the U-turn. Larger DNA particles were deflected less strongly than smaller particles, which contrasts with the findings of other groups [38]. They explained that due to the shallow channel depth employed, that is smaller than the radius of gyration of the DNA particles, DNA particles may be affected by the electric field produced by the Debye layers shielding the channel walls. An important contribution of this study is that the authors explain that the Clausius–Mossotti (CM) factor model does not apply to DNA particles since charge cannot be redistributed because it is fixed on its backbone. Their results

demonstrated an effective method for particle sorting with great potential for analytical applications. Nevertheless, a variety of pharmaceutical and genomic applications would also require particle concentration.

In 2004 Ying *et al.* [34] reported experimental and mathematical work on the trapping of DNA particles employing a nanopipette with AC and DC electric fields. By modeling the electric field gradient along the pipette, it was found that it reached a maximum field of 8000 V/cm at the pipette opening. Same DEP behavior was observed with the 40 mer of ssDNA and dsDNA. At voltages higher than 2 V at a frequency of 0.5 Hz, the electric field gradient generated was enough to achieve DEP trapping of DNA. This technique has a great potential for analytical applications [34].

A summary of the findings on the DEP manipulation and concentration of DNA particles mentioned above is given in Table 1.

### 1.3 Present work

This article describes the DEP trapping and concentration of linear DNA particles (pET28b) employing a microchannel with embedded cylindrical insulating posts and DC electric fields. As mentioned above, iDEP of PCR-amplified ssDNA and dsDNA particles of different sizes has been concentrated and separated with AC electric fields [38], with EP migration with DC and trapping with AC electric fields [45]. Other studies achieved DNA particle sorting [50] and concentration with a nanopipette and DC electric fields [34]. However, to the best knowledge of the authors, the DEP trapping of linear DNA particles, taking advantage of the electroosmotic fluid pumping under DC electric fields, has not been reported yet. In addition, DNA reversible agglomeration under DC electric fields was observed and discussed. Agarose gel analyses are also included to demonstrate that DNA was not denatured by DEP trapping or agglomeration. Moreover, concentration factors (CFs) for DNA particles from 8 up to 24 times the feed concentration were obtained with a processing time of around 2 min, making this technique attractive as a fast tool for sample concentration. This study describes a semi-continuous system that concentrated DNA particles while the suspending medium flows through, allowing for DNA particles to be eluted as a plug of concentrated sample suitable for further analysis and manipulation. These results establish the great capability of iDEP for concentration and manipulation of DNA, opening the possibility for the development of DEP microdevices to be used in genomics and pharmaceutical applications, where rapid concentration and purification of DNA are an immediate need.

## 2 Theory

First proposed by Pohl in 1951, DEP is particle movement due to polarization effects under the presence of a non-uniform electric field; it can occur with both AC and DC

fields [51]. The DEP force exerted on a spherical particle can be defined as:

$$F_{\text{DEP}} = 2\pi\epsilon_m r_p^3 \text{Re}(f_{\text{CM}}) \nabla E^2 \quad (1)$$

where  $\epsilon_m$  is the permittivity of the suspending medium,  $r_p$  is the radius of the particle,  $E$  is the local electric field, and  $\text{Re}(f_{\text{CM}})$  is the real part of the CM factor expressed as:

$$f_{\text{CM}} = \frac{\epsilon_p^* - \epsilon_m^*}{\epsilon_p^* + 2\epsilon_m^*} \quad (2)$$

where  $\epsilon_p^*$  and  $\epsilon_m^*$  are the complex permittivities of the particle and the medium, respectively. The complex permittivity is related to the real permittivity  $\epsilon$  by the expression  $\epsilon^* = \epsilon - (j\sigma/\omega)$ , where  $\sigma$  and  $\omega$  are the conductivity and angular frequency of the applied electric field, respectively, while  $j = \sqrt{-1}$ . The CM accounts for the particle polarizability, a positive value means that the particle is more polarizable than the suspending medium and will be attracted to the regions of higher field intensity. A negative value of CM means that particles are less polarizable than the medium and will be repelled from the regions of higher field intensity. When a DC electric field is used, the CM factor can be expressed in terms of the real conductivities of the particle ( $\sigma_p$ ) and the suspending medium ( $\sigma_m$ ) [52]:

$$f_{\text{CM}} = \frac{\sigma_p - \sigma_m}{\sigma_p + 2\sigma_m} \quad (3)$$

When DC electric fields are employed with iDEP, EP and EOF are also present. EK is the superposition of EP and EOF. For a microchannel with a negative surface charge, such as glass, the EK velocity ( $v_{\text{EK}}$ ) can be defined as follows, considering the net direction of the flow as positive [53]:

$$v_{\text{EK}} = \mu_{\text{EK}} E = (\mu_{\text{EO}} - \mu_{\text{EP}}) E \quad (4)$$

$$v_{\text{EO}} = \mu_{\text{EO}} E \quad (5)$$

$$v_{\text{EP}} = \mu_{\text{EP}} E \quad (6)$$

where  $\mu_{\text{EO}}$  and  $\mu_{\text{EP}}$  are the electroosmotic and EP mobilities, and  $v_{\text{EO}}$  and  $v_{\text{EP}}$  are the electroosmotic and EP velocities, respectively.

In order to achieve trapping of particles, the DEP velocity must overcome that of EK [53]. This is possible only under high electric fields, since the former  $v_{\text{EK}}$  is linearly related to the field, while  $v_{\text{DEP}}$  has a relationship of second order with the applied field:

$$v_{\text{DEP}} = -\mu_{\text{DEP}} \nabla E^2 \quad (7)$$

where  $v_{\text{DEP}}$  and  $\mu_{\text{DEP}}$  are the DEP velocity and mobility, respectively.

## 3 Materials and methods

### 3.1 DNA sample preparation

*Escherichia coli* TOP10F' cells harboring the pET28b(+) (Novagen, Madison, WI, USA) vector (5369 bp) were

**Table 1.** Summary of the results on the DEP manipulation and concentration of DNA particles

Ref.	DEP system	DNA type	Electric field characteristics	Type of DEP response and comments
Zheng <i>et al.</i> [8]	eDEP	dsDNA (45.8 kbp)	AC field 8 V 100 kHz–30 MHz	Positive DEP Golden quadrupole electrodes
Hölzel <i>et al.</i> [33]	eDEP	dsDNA (7.3 kbp)	AC field 3 V 1 MHz	Positive dielectrophoresis Golden interdigitated electrodes
Ying <i>et al.</i> [34]	iDEP	ssDNA (40 mer, 1 kb) and dsDNA (40 mer)	AC/DC field 0.5–4 V 0.1–1000 Hz	Positive DEP Borosilicate glass nanopipette
Du <i>et al.</i> [35]	eDEP	dsDNA (166 kbp)	AC field 5–20 V 1 kHz	Positive DEP Golden asymmetric quadrupole electrodes
Asbury <i>et al.</i> [36]	eDEP	dsDNA (4.4, 35.9, 48.5, and 164 kbp)	AC field 0.5–200 V 30 Hz	Positive DEP Golden interdigitated electrodes
Chou <i>et al.</i> [38]	iDEP	ssDNA (137 nucleotides) and dsDNA (0.37, 40 kbp).	AC field 1 kV 200–1000 Hz	Positive DEP Microdevice made from quartz, trapezoidal insulating structures
Regtmeier <i>et al.</i> [45]	iDEP	ssDNA (48.5, 164 kpb) and dsDNA (7, 14 kpb)	AC field 150–240 V 60 Hz	Positive DEP Microdevice of PDMS, rectangular insulating posts
Chou and Zenhau sern [47]	iDEP	ssDNA (1 kpb) and dsDNA (103 kpb)	AC field 200 V 1 kHz	Positive DEP Channels with constrictions made of polydimethylsiloxane
Parikesit <i>et al.</i> [50]	iDEP	dsDNA (48.5, 165.6 kpb) 0–15.3 V 0–1 MHz	AC/DC field	Negative DEP Glass fluidic channel with a sharp corner

cultured overnight at 37°C in Luria–Bertani media supplemented with kanamycin (50 µg/mL). Plasmidic DNA was extracted from bacteria using PureLink™ HiPure Plasmid Midiprep Kit (Cat. No. K2100-05, Invitrogen, Carlsbad, CA, USA). All purified plasmid DNA was diluted in ultrapure distilled water, free of DNases and RNases (Cat. No. 10977-015, Invitrogen). Linearization of plasmid DNA was achieved by selective cleavage using *Hind*III restriction endonuclease (New England Biolabs, Ipswich, MA, USA). Linear DNA was then precipitated by adding 10 and 250% of the solution volume of CH<sub>3</sub>COONa 3 M and ice-cold ethanol 95%, respectively. Then followed by centrifugation (14 000 × *g* for 20 min) [54]. The supernatant was discarded and the precipitated DNA was washed with 70% ethanol and centrifuged a second time (14 000 × *g* for 10 min). The dried pellet was resuspended in water to the desired concentration.

DNA concentrations were measured by absorbance at 260 nm, and general purity assessed by an UV-scan from 220 to 320 nm using NanoDrop™1000 spectrophotometer (Thermo Scientific, Waltham, MA, USA). Fluorescent staining of DNA was done with Syto 9® excitation/emission 483/503 nm (Invitrogen), which was added to the DNA sample at a ratio of ~1 Syto molecule for every 2 bp, and incubated 5 min prior to sample loading.

### 3.2 Microdevice

A set of experiments was carried out employing a microdevice made from D263 borosilicate glass substrates; a schematic representation is shown in Fig. 1. The microdevice is conformed by a top substrate with reservoirs and a bottom substrate with channels. The microchannel used for experimentation is 10.16 mm long, 2 mm wide, and 7 µm deep and contains an array of cylindrical posts straddled by the inlet and outlet reservoirs. The posts had a diameter of 470 µm, arranged 510 µm center-to-center. The post array had a total of 32 cylindrical posts, arranged in eight columns of four posts each. The first column of posts on either side has a “dove tail” geometry to prevent particles from colliding against the posts and plugging the system. The microdevice was fabricated as follows: a 300 nm-thick layer of SiC was deposited on substrates by plasma-enhanced chemical vapor deposition, which served as hard mask for the microchannels on the bottom substrate. Then, wafers were spin coated with positive photoresist and soft-baked at 100°C for 15 min. Mask pattern was transferred by exposure to UV light. After exposure and developing photoresist layer, substrates were hard-baked at 90°C for 15 min. SiC was dry etched by using CF<sub>4</sub> plasma in a reactive ion etching system, exposing the glass, 7 µm were subsequently wet etched in a HF:HCl

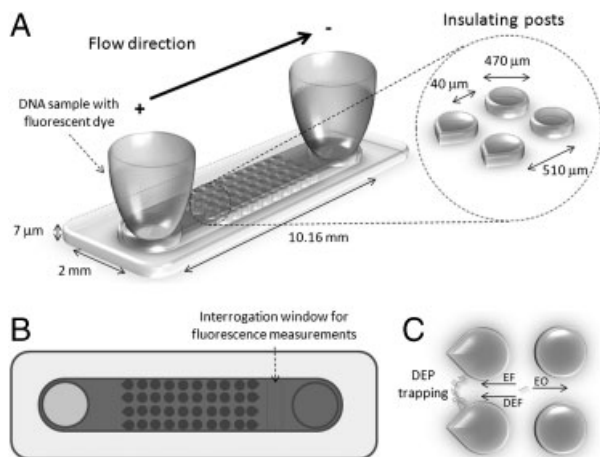


**Figure 1.** Schematic representation of equipment setup for iDEP experimentation. (A) 3-Dimensional representation of the microchannel employed. (B) 2-Dimensional representation of the microchannel depicting the interrogation window employed for fluorescence measurements for CF estimations. (C) Representation of the forces acting on the DNA particles. EP and DEP forces are directed against the EOF.

solution, followed by the removal of the mask material. Reservoirs on the top wafer were drilled employing diamond-tipped drill bits, producing reservoirs with an approximated diameter of 1 mm and a volume of 0.864 mL. To clean and prepare the surface for bonding, piranha solution ( $\text{HSO}_4$ :  $\text{H}_2\text{O}_2$  at  $100^\circ\text{C}$ ), HF dip (2%), and NaOH (40% at  $80^\circ\text{C}$ ), were used. As a final step, top and bottom substrates were aligned and thermally bonded at  $610^\circ\text{C}$  for 5 h.

### 3.3 Suspending medium

Suspending media were prepared from bidistilled water; conductivity and pH were measured and adjusted to desired values in the following ranges: 100–120  $\mu\text{S}/\text{cm}$  for conductivity and 10.8–11.15 for pH by adding NaOH and  $\text{KH}_2\text{PO}_4$ . Additionally, Tween-20 and triethanolamine (TEA) were added to the media as DNA stabilizers reaching concentrations of 1.5% and 1.5 M, respectively.

### 3.4 Equipment

DC electric fields were applied using a 3000 V high-voltage sequencer, model HVS448 (LabSmith, Livermore, CA, USA) by employing platinum-wire electrodes with a diameter of 0.3048 mm (Omega, Stamford, CT, USA) placed at each of the reservoirs. DEP behavior of DNA particles was recorded in the form of video and pictures by utilizing an inverted epifluorescence video microscope for microfluidics, model SVM340 (LabSmith). A 4X microscope objective was employed for all experiments. The microscope has a light module that emits blue light, which excites at a wavelength of 480 nm. The filter configuration of the microscope allows

detecting light emissions above a wavelength of 515 nm. Both the high voltage sequencer and the microfluidics microscope require the use of a personal computer for their operation.

### 3.5 CF estimations

CF of the DNA sample employing iDEP was evaluated by performing fluorescence measurements in an interrogation window located just after the outlet of the post array as shown in Fig. 1B. A set of experiments was performed, using the following steps:

(i) After the sample was introduced into the microchannel, EOF was generated by applying a low voltage of 200 V/cm for 10 s to record and measure the fluorescence of the moving sample of linear pET28b DNA as it came out of the post array. (ii) Then the applied field was increased to 2000 V/cm for 20 or 40 s in order to dielectrophoretically trap DNA particles; low-fluorescence measurements at the interrogation window were obtained during this high electric field treatment, since most of the DNA particles were immobilized at the post array, and not many DNA particles passed through the interrogation window. (iii) Finally, the field was lowered back to 200 V/cm, in order to release the concentrated particles from the DEP traps, by means of EOF and pushing the plug of particles through the interrogation window resulting in an increase of the fluorescence signal. Fluorescence measurements to determine the CF during the process were obtained using software built in house, by selecting an interrogation window located just after the outlet of the post array, as shown in Fig. 1B. CF is determined by dividing the maximum fluorescence value of the plug of concentrated sample (CP) by the fluorescence signal of the sample before DEP trapping (CB):

$$\text{CF} = \frac{\text{CP}}{\text{CB}} \quad (8)$$

A high CF value can be related to a more efficient trapping of DNA particles, and therefore represents the process capability to achieve concentration.

### 3.6 Procedure for DEP trapping experiments

Prior to each iDEP experiment, the microdevice was cleaned with bidistilled water and filled with the suspending medium. A sample of 30  $\mu\text{L}$  of DNA at a concentration of 50  $\mu\text{g}/\text{mL}$  was introduced at the inlet reservoir. Care was taken to eliminate pressure-driven flow after the electrodes were placed at the inlet and outlet reservoirs in order to apply a DC electric field. The DEP response of the particles was recorded employing the microscope in the form of videos and pictures.

### 3.7 Gel analysis

In order to assess the integrity of the DNA during experimentations, agarose gel EP was conducted as described by Sambrook and Russell [55] using 0.7% agarose gels

containing 0.5  $\mu\text{g/mL}$  ethidium bromide. Gels were placed on Tris-acetate-EDTA buffer (pH = 9,  $\sigma_m = 460 \mu\text{S/cm}$ ) and ran for 1 h at an approximated field of 7 V/cm generated by a model 200/2.0 power supply (Bio-Rad, Hercules, CA, USA).

## 4 Results and discussion

### 4.1 DEP trapping of DNA particles

From Eqs. (4) and (7), it can be deduced that while the EK forces relate linearly to the applied electric field, the DEP force has a second-order dependency. This means that for higher applied fields DEP will overcome EK, as discussed earlier. In the case of these experiments, since DNA is negatively charged, due to its sugar-phosphate backbone, DNA EP migration will occur from the negative to the positive electrode (toward the microchannel inlet reservoir). When DC fields are applied, the majority of bioparticles will exhibit negative DEP behavior [53], *i.e.* particles are less polarizable than the suspending medium and will be repelled from the regions of higher field intensity. As mentioned by Parikesit *et al.* [50] DNA polarization is a complex phenomena that cannot be simply described by the CM factor model. Our experimental observations, as it is shown below, demonstrated negative DEP trapping of DNA. Majority of the studies on iDEP of DNA have reported positive DEP trapping obtained with AC electric fields [38, 45]. Only Tsukahara *et al.* [56] reported negative DEP trapping of DNA with planar quadrupole electrodes. In our system DC electric fields are employed where DNA follows a different mechanism than that of obtained with AC electric fields.

The main forces present in our system are DEP, EOF and EP. Representation of these three forces is shown in Fig. 1C. In our experiments, DNA particles exhibit negative DEP, *i.e.* DNA particles are repelled from the narrow regions between the posts (zone with higher field intensity) causing a DEP net movement in the direction of the inlet reservoir. The only EK force that will promote movement toward the outlet reservoir will be EOF. It should be noted that according to the charge–mass ratio of DNA, EP force is significant when compared with electroosmotic force, and it should be considered. From the previous studies with particle imaging velocimetry measurements performed employing micro-devices made from the same glass material, and under similar operating conditions, but lower pH (pH = 9); it was determined that the average electroosmotic mobility was around  $1.75 \times 10^{-4} \text{ cm}^2/\text{Vs}$  [53]. The pH value employed in this study for DEP trapping of DNA is pH = 11.15, at a higher pH value, a greater electroosmotic mobility is expected, as it has been reported earlier [53]. By performing a simple extrapolation from the values reported [53], an electroosmotic mobility of around  $2 \times 10^{-4} \text{ cm}^2/\text{Vs}$  can be expected for these operating conditions of pH = 11.15.

Values for EP mobility of DNA molecules were determined to be around  $0.72\text{--}1.1 \times 10^{-4} \text{ cm}^2/\text{Vs}$  for solution with a low ionic strength employing the Henry equation

[57]. As one can see the values for electroosmotic and EP mobilities are in the same order of magnitude, however, electroosmotic mobility in our system is greater than EP mobility, resulting in an EK flow toward the outlet reservoir, as it was observed.

In accordance to the theory, under low applied fields, when DEP is negligible, EOF will dominate the system and sample will move from the positive to the negative electrode [40, 53]. As the electric field is increased, weak trapping will occur as DEP and EK forces struggle to overcome each other. When the applied field is sufficiently strong, DEP force will be great enough to overcome EK, and then DNA particles will be negatively dielectrophoretically immobilized, forming a band of trapped particles prior to the regions of higher field intensity (narrow regions between the cylindrical posts). During this time, DNA particles will concentrate at different DEP traps until the field is lowered to release the particles from the traps. Figure 2 shows a sequence of images depicting this dielectrophoretic behavior. These results were obtained employing a suspending medium with  $\sigma_m = 104 \mu\text{S/cm}$  and pH of 11.15. Figure 2A shows DNA particles flowing with EOF under a field of 500 V/cm, where some DEP effect is observed at the constriction. Negative DEP trapping of DNA particles was clearly observed by increasing the applied field to 1000 V/cm (Fig. 2B), where “waves” of repelled particles occurred. Strong DNA trapping is achieved when the field is increased to 1500 V/cm (Fig. 2C), observing even stronger “waves” of repelled particles. As one can see from these results, successful DNA immobilization due to negative DEP trapping is obtained, that increases with the applied field. Experiments for DEP trapping were repeated at least three to five times each, obtaining excellent reproducibility.

Due to the small size of DNA particles, high applied fields are required, as DEP force is directly proportional to  $r_p^3$ , these high fields can cause DNA degradation. Agarose gel EP analyses were performed with samples extracted from the inlet and outlet reservoirs of the microchannel. Figure 2D presents the results of these analyses, showing that denaturalization and/or degradation of the sample is negligible under the strong electric fields employed.

Regarding the direction of the EK flow, it is from left to right, *i.e.* from the inlet to the outlet reservoir. This is confirmed by the position of the band of trapped DNA particles in Figs. 2A–C (negative DEP), where the band of immobilized DNA particles is formed just before to the left side of the constriction, just before the narrow region between the cylindrical posts. If the EK flow had been from right to left, the band of trapped particles would have been formed to the right side of the constriction.

### 4.2 DNA particle aggregation induced by electric fields

During experimentation it was observed that DNA aggregates were formed while the electric field was applied. This

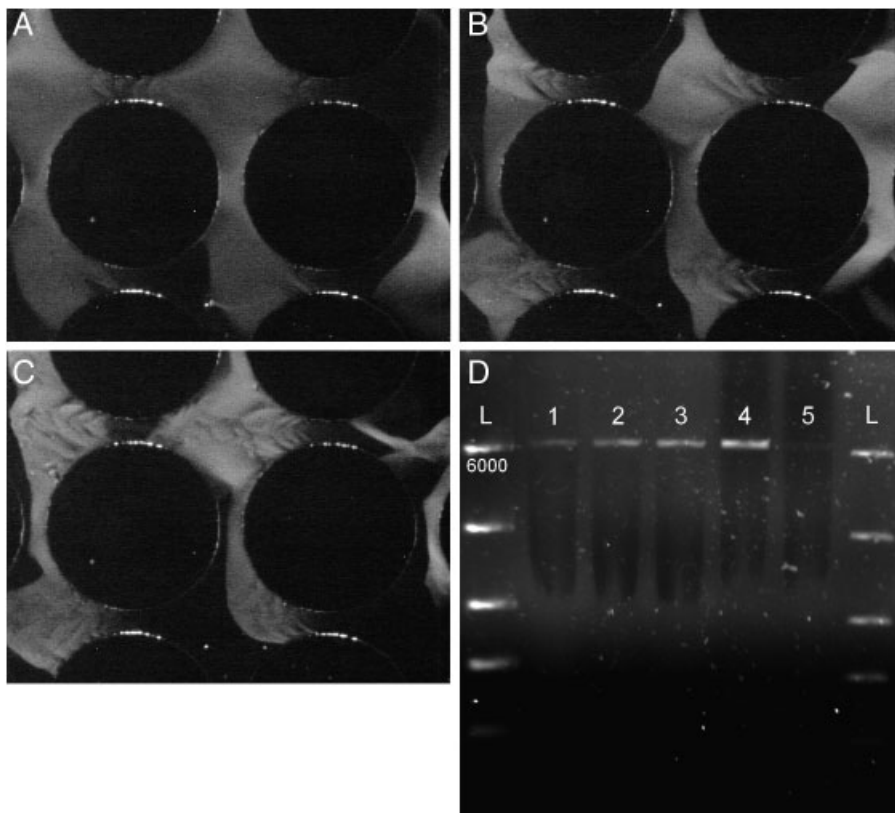


**Figure 2.** DEP trapping of linear DNA (pET28b) employing a suspending medium with 1.5 M TEA and 1.5% Tween-20, with conductivity of  $104 \mu\text{S}/\text{cm}$  and a pH of 11.15. (A) DNA particles immobilized due to negative DEP at a field of  $500 \text{ V}/\text{cm}$ . (B) Stronger DEP trapping of DNA particles when a field is increased to  $1000 \text{ V}/\text{cm}$ , picture shows weak “waves” of DNA particles caused by particles being repelled from the narrow region between the posts. (C) Strong DEP trapping of DNA particles demonstrated by very intense fluorescence when a field of  $1500 \text{ V}/\text{cm}$  is applied, showing stronger “waves” of repelled DNA particles. (D) Agarose gel EP of linear DNA particles as follows: ladder (L), DNA stock (1), dyed DNA stock (2), inlet reservoir (3), sample recovered from the post array (4), sample recovered from outlet reservoir (5). Well-defined bands at the same molecular weight (5.3 Kbp) show that DNA was not broken or denatured by DEP trapping (molecular weight of the ladder is shown left).

phenomenon was predominant at the narrow regions between the posts. Such aggregates were proportional in size to the intensity of the applied electric field. After the field was removed, the aggregates were clearly dispersed aided by the usage of stabilizers (TEA and Tween-20). Previous experiments carried out with absence or lower concentration of TEA and Tween-20, consistently formed larger aggregates that did not disperse after removing the electric field. In addition, lack of TEA and Tween-20 caused significant DNA degradation.

Figure 3 shows a sequence of images where DNA aggregates are formed and then dispersed as a function of time and the applied field. Suspending medium used for these experiments had a conductivity of  $120 \mu\text{S}/\text{cm}$  and a pH of 10.8. Figure 3A shows DEP behavior obtained 0.7 s after a field of  $2000 \text{ V}/\text{cm}$  was applied, where aggregates start to form at the region with maximum field intensity (narrow region between posts). Figure 3B, taken 3.5 s after applying the field, shows fully developed agglomerates that are flowing through the channel. Immediately after removing the applied field ( $0 \text{ V}/\text{cm}$ ), aggregates disperse as shown in Figs. 3C and D, where the former was taken 0.1 s when the field was removed, and the latter was obtained 1.1 s later. Agarose gel EP analysis (Fig. 4) reveals that aggregates are neither a result nor a cause of DNA degradation or denaturalization; since the band of DNA sample extracted from the microchannel outlet (Fig. 4, lane 4) is clearly defined and migrates at the same molecular

weight than the original DNA stock (Fig. 4, lanes 1 and 2). Aggregate size depends on the magnitude of the applied electric field as shown in Figs. 5A and B, where it can be observed that at  $500 \text{ V}/\text{cm}$  (Fig. 5A) tiny aggregates are formed; and much larger aggregates are obtained by increasing the field to  $1500 \text{ V}/\text{cm}$  (Fig. 5B). Additionally, the largest aggregates found in our experiments were obtained at  $2000 \text{ V}/\text{cm}$  (Fig. 3B).

Some studies on DNA separation by capillary EP have reported formation of DNA aggregates at high field strengths and low frequencies [58, 59]. Song and Maestre reported [58] snow-ball-shaped DNA aggregates formed at applied fields above  $400 \text{ V}/\text{cm}$ . Mitnik *et al.* [59] suggested that dipole–dipole interactions may be the main cause for DNA aggregations, causing electrohydrodynamic instability. This phenomenon was observed on DNA segregated in capillaries when AC fields were applied, and, similar to our own observations, DNA aggregation increased with the applied field. However, aggregates re-dispersed after a few hours of stopping the field [59] (in our experiments, DNA conglomerates dispersed completely in about 1 s, see Fig. 3D). Interestingly, later it was reported that high-magnitude electric pulses can cause a shift in the conformation  $A \leftrightarrow B$  equilibrium toward DNA to B form, this being driven by dipolar stretching of the molecule [60], supporting the results obtained by Mitnik *et al.* [59]. The above findings may suggest that DNA aggregates in our system are the results of dipole–dipole interactions occurred

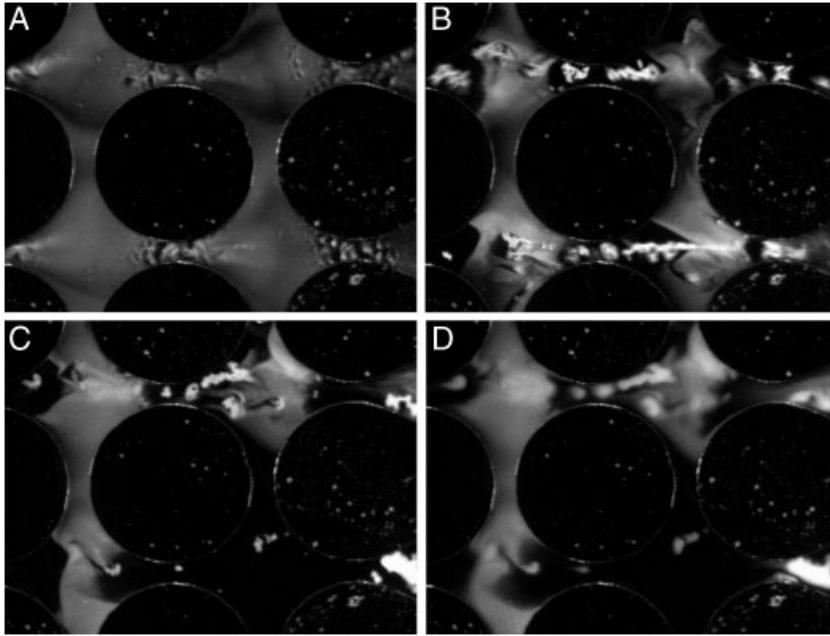


**Figure 3.** Sequence of images showing DNA aggregates formed by applying an electric field and then dispersing after the field was removed, employing a suspending medium of  $\sigma_m = 120 \mu\text{S}/\text{cm}$  and  $\text{pH} = 10.8$ . (A) Image showing aggregates starting to form by applying a field of  $2000 \text{ V}/\text{cm}$ , image was taken  $0.7 \text{ s}$  after the field was applied, (B) image showing DNA aggregates fully formed at a field of  $2000 \text{ V}/\text{cm}$ , image was taken  $3.5 \text{ s}$  after the field was applied; (C)  $0.1 \text{ s}$  after the field was removed, aggregates start to disperse; and (D) at  $1.1 \text{ s}$  after removing the field, fully dispersed aggregates are observed.

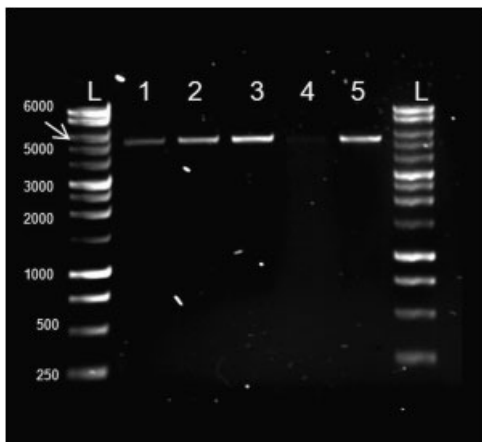


**Figure 4.** Agarose gel EP of linear DNA particles as follows: ladder (L), DNA stock (1), dyed DNA stock (2), inlet reservoir (3), sample recovered from outlet reservoir (4), sample recovered from the post array (5). Molecular weight of the ladder is shown left. From these gel results it can be observed that DNA particles (including the re-dispersed aggregates) were not denatured by DEP.

at the regions of electric field maxima (narrow regions). High electric fields favor conformation shift toward B form of DNA molecules, which possesses a higher effective dipole moment that may lead to the generation of aggregates. Jose and Porschke [60] employed short and extremely intense electric pulses in the range of  $10\text{--}50 \text{ kV}/\text{cm}$  to achieve the DNA conformational shift A  $\rightarrow$  B. In our system, aggregates formation occurred at the regions of field maxima, where the field reaches from  $2.5$  to  $15 \text{ kV}/\text{cm}$ , given the fivefold increase due to electric field non-uniformity showed by mathematical modeling [53].

### 4.3 Determination of CFs of DNA particles

Process efficiency can be determined in terms of CF, which relates the concentration of DNA particles reached after DEP trapping. As mentioned in Section 3, DNA concentration was measured employing fluorescence signals. Figure 6A shows the fluorescence measurements obtained by following the procedure described in Section 2. First, a field  $200 \text{ V}/\text{cm}$  was applied for  $5 \text{ s}$ , where the average fluorescence obtained was  $1.5$  (arbitrary units of fluorescence), which should correspond to a DNA concentration of  $50 \mu\text{g}/\text{mL}$ . Then, the field was increased to  $2000 \text{ V}/\text{cm}$ , employing two different processing times of  $20$  or  $40 \text{ s}$ , this higher field was applied to achieve DEP trapping and concentrate DNA particles. Then, the applied field was lowered back to  $200 \text{ V}/\text{cm}$  to release the plug of concentrated particles and measure the increase in fluorescence. A fluorescence peak was obtained, with a maximum fluorescence values of  $12.31$  and  $36.69$  (arbitrary units) for concentration times of  $20$  and  $40 \text{ s}$ , respectively. From these fluorescence measurements and employing Eq. (8), the CFs of  $8.20$  and  $24.46$  were calculated ( $20$  and  $40 \text{ s}$  concentration time, respectively), more than an order of magnitude increase compared with feed concentration. This means that the DNA released from the posts was from  $8$  up to  $24$  times more concentrated than the original sample. Considering that the feed concentration was  $50 \mu\text{g}/\text{mL}$ , the maximum peak concentration obtained was around  $1200 \mu\text{g}/\text{mL}$ . These CF values were obtained employing a suspending medium with a conductivity of  $104 \mu\text{S}/\text{cm}$  and  $\text{pH}$  of  $10.8$ . According to Du *et al.* [35], there is a non-linear relationship between DNA concentration and fluorescence, *i.e.* the fluorescence signal obtained does not increase linearly with DNA concentration; fluorescence increases to lesser extent. Therefore, the CF measured with fluorescence is lower than the real CF obtained

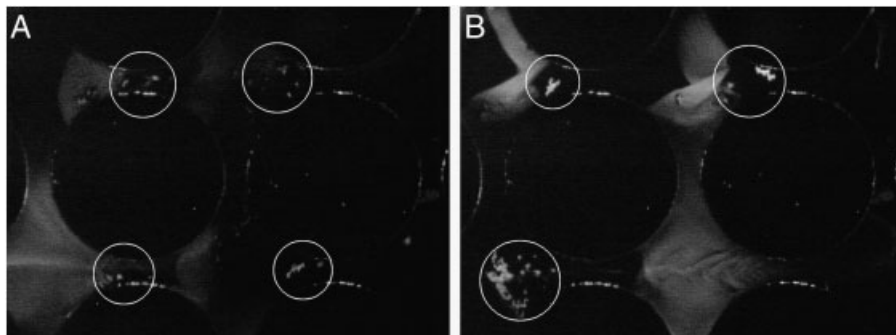


**Figure 5.** Aggregate size dependence on electric field magnitude. (A) Tiny aggregates formed at an applied field of 500 V/cm; (B) formation of larger aggregates at an applied field of 1500 V/cm.

[35]; this means that our experiments could have produced even higher CFs than the values we are reporting. It is important to note that DNA particle concentration was achieved with processing times of around 2 min (Fig. 6A). This fast concentration process represents a significant advantage over traditional laboratory techniques for DNA concentration such as DNA precipitation and lyophilization.

In order to assess whether DNA particles were denatured during CF measurements, samples taken from the microchannel outlet were analyzed by gel EP. Figs. 6B and C show the results for the samples obtained after 20 and 40 s of processing time, respectively. It can be seen in lane 6 of both gel EP results (Figs. 6B and C) that DNA bands are well defined and migrated at the same velocity than that of the stock DNA solution, thus DNA particles did not get denatured as a result from concentration experiments.

Furthermore, an additional control experiment was performed in order to confirm that the formation of DNA aggregates was from DNA particles and not from the presence of contamination and/or dye particles. A field of 500–1500 V/cm was applied to the microchannel employing the same suspending medium used for CF estimation ( $\sigma_m = 104 \mu\text{S}/\text{cm}$ , pH = 11.15) with the addition of 1.5 M TEA, 1.5% Tween-20, and the fluorescent dye, but without the DNA sample. During this control neither the DEP trapping of the dye nor the presence of aggregates was observed (data not shown). These results confirmed that sample concentration and aggregate formation shown in Figs. 2 and 3 were DNA particles.

## 5 Concluding remarks

This research work presents the manipulation and concentration of linear DNA particles (pET28b) with iDEP. The microchannel employed was made from glass and contained an array of cylindrical insulating structures. DC electric fields were employed allowing for EOF to pump the flow across the microchannel.

Suspending mediums with conductivities between 100 and 120  $\mu\text{S}/\text{cm}$  and pH of 10.8–11.15 were employed for the DEP trapping of DNA particles with applied fields between 500 and 1500 V/cm. Tween-20 and TEA were added to the suspending medium as DNA stabilizers. Experimental results

showed that by varying the magnitude of the applied field it was possible to control the degree of negative DEP trapping, from DNA particles under weak trapping or particles exhibiting strong trapping, suitable to achieve significant sample concentration. These results demonstrated that balancing EP, electroosmotic, and DEP forces allow for control of DNA particle manipulation by adjusting operating conditions, such as the magnitude of the applied DC electric field.

The formation of DNA aggregates was observed to increase at higher applied fields; however, this phenomenon was reversible since conglomerates dispersed immediately once the field was removed. DNA particles were not denatured with this process as demonstrated by gel EP analysis.

In order to test the potential of this system for concentration of DNA, the CFs achieved by applying a field of 2000 V/cm for processing times of 20 and 40 s were measured employing fluorescence. It was found that the systems can increase sample concentration up to 24 times.

iDEP is still a nascent technique, and its application has just started to grow. Majority of the research work with iDEP has been done with micro-bioparticles, such as bacteria, yeast, and mammalian cells. Only few reported applications exist where nano-bioparticles were manipulated with iDEP.

The results obtained from this study demonstrate that simple iDEP systems, such as microchannel with cylindrical posts, can be employed to manipulate small DNA particles using a combination of electroosmotic, EP, and DEP forces. Concentration of DNA particles, at a different level of DEP trapping, with our basic system was demonstrated. CFs of DNA samples were also estimated, confirming the great potential of this technique for bioparticle concentration. These findings establish the potential that iDEP has to offer for the manipulation of nano-bioparticles, such as DNA. It is expected that further development of iDEP will make a significant impact on many biotechnological fields, such as gene therapy and DNA vaccines.

*The authors acknowledge the financial support provided by the grant CONACYT-CB-2006-53603. The authors are grateful for the financial support provided by Cátedras de Investigación (CAT122 and CAT142) of Tecnológico de Monterrey.*

*The authors have declared no conflict of interest.*

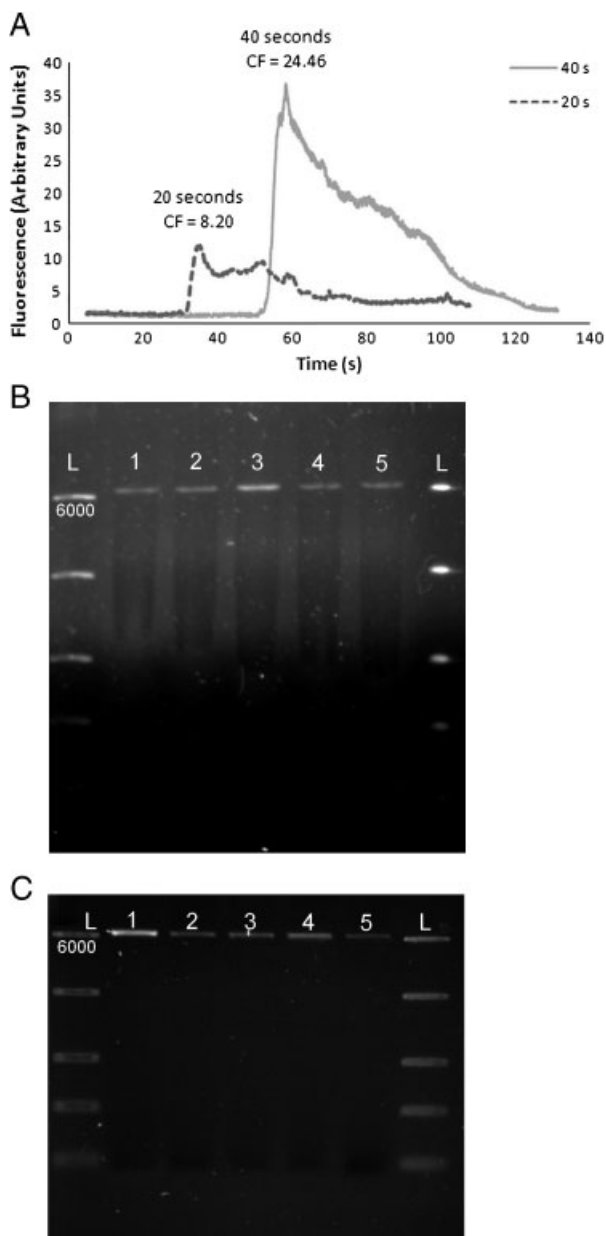


**Figure 6.** Fluorescence measurements of CF of DNA particles. (A) Fluorescence as a function of time; (B) agarose gel EP analysis of sample after 20 s of at a field of 2000 V/cm; (C) agarose gel EP analysis of sample after 40 s of at a field of 2000 V/cm. Lanes are numbered as in Fig. 2D. These results demonstrate that DNA particles were not denatured.

## 6 References

[1] Gardeniers, H., Van Den Berg, A., *Int. J. Environ. Anal. Chem.* 2004, **84**, 809–819.  
 [2] Escarpa, A., González, M. C., López-Gil, M. A., Crevillén, A. G., Hervás, M., García, M., *Electrophoresis* 2008, **29**, 4852–4861.  
 [3] Kang, L., Chung, B. G., Langer, R., Khademhosseini, A., *Drug Discov. Today* 2008, **13**, 1–13.

[4] Whitesides, G. M., *Nature* 2006, **442**, 368–373.  
 [5] Gonzalez, C. F., Remcho, V. T., *J. Chromatogr. A* 2005, **1079**, 59–68.  
 [6] Clarke, R. W., White, S. S., Zhou, D., Ying, L., Klenerman, D., *Angew. Chem.* 2005, **44**, 3747–3750.  
 [7] Lapizco-Encinas, B. H., Ozuna-Chacón, S., Rito-Palmares, M., *J. Chromatogr. A* 2008, **1206**, 45–51.  
 [8] Zheng, L. F., Brody, J. P., Burke, P. J., *Biosens. Bioelectron.* 2004, **20**, 606–619.  
 [9] Bakewell, D. J., Morgan, H., *IEEE Trans. Nanobios.* 2006, **5**, 1–8.  
 [10] Hölzel, R., Bier, F. F., *IEEE Proc. Nanobiotechnol.* 2003, **150**, 47–53.  
 [11] Washizu, M., *J. Phys. Conf. Ser.* 2003, **178**, 89–94.  
 [12] Ermolina, I., Milner, J., Morgan, H., *Electrophoresis* 2006, **27**, 3939–3948.  
 [13] Akin, D., Li, H., Bashir, R., *Nano Lett.* 2004, **4**, 257–259.  
 [14] Lapizco-Encinas, B. H., Simmons, B. A., Cummings, E. B., Fintschenko, Y., *Anal. Chem.* 2004, **76**, 1571–1579.  
 [15] Suehiro, J., Hamada, R., Noutomi, D., Shutou, M., Hara, M., *J. Electrostatics* 2003, **57**, 157–168.  
 [16] Li, H., Bashir, R., *Sens. Actuat. B Chem.* 2002, **86**, 215–221.  
 [17] Markx, G. H., Talary, M. S., Pethig, R., *J. Biotechnol.* 1994, **32**, 29–37.  
 [18] Altomare, L., Borgatti, M., Medoro, G., Manaresi, N., Tartagni, M., Guerrieri, R., Gambari, R., *Biotechnol. Bioeng.* 2003, **82**, 474–479.  
 [19] Yu, C. H., Vykoukal, J., Vykoukal, D. M., Schwartz, J. A., Shi, L., Gascoyne, P. R. C., *J. Microelectromech. Sys.* 2005, **14**, 480–487.  
 [20] Sankaran, B., Racic, M., Tona, A., Rao, M. V., Gaitan, M., Forry, S. P., *Electrophoresis* 2008, **29**, 5047–5054.  
 [21] Srivastava, S. K., Daggolu, P. R., Burgess, S. C., Minerick, A. R., *Electrophoresis* 2008, **29**, 5033–5046.  
 [22] Brown, A. P., Betts, W. B., in: Smith, M., Thompson, K. C. (Eds.), *Cryptosporidium: The Analytical Challenge*, Royal Society of Chemistry (Special Publication), Coventry, England 2001, pp. 84–87.  
 [23] Prazeres, D. M. F., Ferreira, G. N. M., Monteiro, G. A., Cooney, C. L., Cabral, J. M. S., *Trends Biotechnol.* 1999, **17**, 169–174.  
 [24] Danquah, M. K., Forde, G. M., *J. Chromatogr. A* 2008, **1188**, 227–233.  
 [25] Levy, M. S., O’Kennedy, R. D., Ayazi-Shamlou, P., Dunnill, P., *Trends Biotechnol.* 2000, **18**, 296–305.  
 [26] Guerrero-Germán, P., Prazeres, D., Guzmán, R., Montesinos-Cisneros, R., Tejada-Mansir, A., *Bioproc. Biosys. Eng.* 2009, **32**, 615–623.  
 [27] Levy, M., Collins, I., Yim, S., Ward, J., Titchener-Hooker, N., Shamlou, P., Dunnill, P., *Bioproc. Bioeng.* 1999, **20**, 7–13.  
 [28] Li, S.-D., Huang, L., *Gene Ther.* 2006, **13**, 1313–1319.  
 [29] Rice, J., Ottensmeier, C. H., Stevenson, F. K., *Nat. Rev. Cancer* 2008, **8**, 108–120.  
 [30] Donnelly, J. J., Wahren, B., Liu, M. A., *J. Immunol.* 2005, **175**, 633–639.

- [31] Freitas, S., Santos, J. L., Prazeres, D. M. F., in: Biber, A., Heinzle, E., Cooney, C. (Eds.), *Development of Sustainable Bioprocesses: Modeling and Assessment*, Wiley, New York, 2006, pp. 271–285.
- [32] Bower, D., Prather, K., *Appl. Microbiol. Biotechnol.* 2009, 82, 805–813.
- [33] Hölzel, R., Gajovic-Eichelmann, N., Bier, F. F., *Biosens. Bioelectron.* 2003, 18, 555–564.
- [34] Ying, L. M., White, S. S., Bruckbauer, A., Meadows, L., Korchev, Y. E., Klenerman, D., *Biophys. J.* 2004, 86, 1018–1027.
- [35] Du, J.-R., Juang, Y.-J., Wu, J.-T., Wei, H.-H., *Biomicrofluidics* 2008, 2, 044103, 1–10.
- [36] Asbury, C. L., Diercks, A. H., van den Engh, G., *Electrophoresis* 2002, 23, 2658–2666.
- [37] Lapizco-Encinas, B. H., Rito-Palomares, M., *Electrophoresis* 2007, 28, 4521–4538.
- [38] Chou, C. F., Tegenfeldt, J. O., Bakajin, O., Chan, S. S., Cox, E. C., Darnton, N., Duke, T., Austin, R. H., *Biophys. J.* 2002, 83, 2170–2179.
- [39] Kang, Y., Li, D., Kalams, S., Eid, J., *Biomed. Microdev.* 2008, 10, 243–249.
- [40] Cummings, E. B., Singh, A. K., *Anal. Chem.* 2003, 75, 4724–4731.
- [41] Thwar, P. K., Linderman, J. L., Burns, M. A., *Electrophoresis* 2007, 28, 4572–4581.
- [42] Gencoglu, A., Minerick, A. R., *Lab Chip* 2009, 9, 1866–1873.
- [43] Suehiro, J., Zhou, G. B., Imamura, M., Hara, M., *IEEE Trans. Ind. Appl.* 2003, 39, 1514–1521.
- [44] Lapizco-Encinas, B. H., Davalos, R., Simmons, B. A., Cummings, E. B., Fintschenko, Y., *J. Microbiol. Methods* 2005, 62, 317–326.
- [45] Regtmeier, J., Duong, T. T., Eichhorn, R., Anselmetti, D., Ros, A., *Anal. Chem.* 2007, 79, 3925–3932.
- [46] Pysker, M. D., Hayes, M. A., *Anal. Chem.* 2007, 79, 4552–4557.
- [47] Chou, C. F., Zenhausern, F., *IEEE Eng. Med. Biol. Mag.* 2003, 22, 62–67.
- [48] Ajdari, A., Prost, J., *Proc. Natl. Acad. Sci. USA* 1991, 88, 4468–4471.
- [49] Warrick, J., Meyvantsson, I., Ju, J., Beebe, D., *Lab Chip* 2007, 7, 316–321.
- [50] Parikesit, G. O. F., Markesteijn, A. P., Piciu, O. M., Bossche, A., Westerweel, J., Young, I. T., Garini, Y., *Biomicrofluidics* 2008, 2, 024103–024114.
- [51] Pohl, H. A., *J. Appl. Phys.* 1951, 22, 869–871.
- [52] Benguigui, L., Lin, I. J., *J. Appl. Phys.* 1984, 56, 3294–3297.
- [53] Martínez-López, J. I., Moncada-Hernández, H., Baylon-Cardiel, J. L., Martínez-Chapa, S. O., Rito-Palomares, M., Lapizco-Encinas, B. H., *Anal. Bioanal. Chem.* 2009, 394, 293–302.
- [54] Altermann, E., Russell, W. M., Azcarate-Peril, M. A., Barrangou, R., Buck, B. L., McAuliffe, O., Souther, N. et al., *Proc. Natl. Acad. Sci. USA* 2005, 102, 3906–3912.
- [55] Sambrook, J., Russell, D., *Molecular Cloning: A Laboratory Manual*, Cold Spring Harbor Laboratory Press, New York, NY 2001.
- [56] Tsukahara, S., Yamanaka, K., Watarai, H., *Chem. Lett.* 2001, 30, 250–251.
- [57] Stellwagen, E., Stellwagen, N., *Biophys. J.* 2003, 84, 1855–1866.
- [58] Song, L., Maestre, M. F., *J. Biomol. Struct. Dyn.* 1991, 9, 525–536.
- [59] Mitnik, L., Heller, C., Prost, J., Viovy, J. L., *Science* 267, 219–222.
- [60] Jose, D., Porschke, D., *Nucleic Acids Res.* 2004, 32, 2251–2258.